Journal of the European Ceramic Society 20 (2000) 715–723

Combustion-synthesis of $SrTiO_3$ Part II. Sintering behaviour and surface characterization

J. Poth, R. Haberkorn, H.P. Beck*

Department of Inorganic and Analytical Chemistry and Radiochemistry, University of Saarland, 66123 Saarbruecken, Im Stadtwald, Gebaeude 23.1, Germany

Received 22 April 1999; received in revised form 24 June 1999; accepted 3 July 1999

Abstract

Nanocrystalline powders of $SrTiO_3$ prepared via combustion-synthesis were sintered at 800 resp. 1000°C. The powders exhibited different grain growth velocities which were measured via X-ray diffraction (XRD). The existence of different $SrCO_3$-species was found by Fourier-transform infrared spectroscopy (FTIR). These could be assigned either to bulk- or surface-$SrCO_3$-species which could be proved by their different decomposition temperatures in thermogravimetry combined with mass spectrometry (TG/MS). A dependence between the grain growth velocities and the existence of surface-$SrCO_3$-species was found: samples which develop surface carbonate species for longer times during sintering will exhibit faster growth rates than samples which showed these species for shorter times. The surfaces of the crystallites are predominantly SrO-terminated which is in agreement with former results of other authors. The strong variations in sintering behaviour caused by only small differences between various samples are typical for nanocrystalline materials, they may be prepared by sol–gel or combustion-synthesis.

Keywords: Combustion synthesis; Grain growth; Sintering; $SrTiO_3$; Surfaces; Titanates

1. Introduction

The sintering behaviour of ceramics is a subject of great importance especially in view of the mechanical properties of the resulting ceramic body. The number of both theoretical and practical work is large; a good overview is given by Brook.[1] The development of the crystallite sizes, for instance, is crucial for the electrical properties of ceramics.[2–4] To change these electrical properties in a controlled manner, doping with different impurities is often made.[5–7] Such additives naturally change the sintering behaviour of the ceramic and decrease or increase the growth rates.[8,9] It is, therefore, important to examine the sintering behaviour thoroughly to gain control over the desired properties of the ceramic body.

An enhancement in crystallite growth is mostly achieved by introducing liquid phases into the grain boundaries; in the case of the earth alkaline titanates, an addition of TiO_2 to approach the respective Ti-rich eutectics (at 1320°C for $BaTiO_3$ and 1440°C for $SrTiO_3$) or SiO_2 and Al_2O_3[10] are used to form such liquid phases.

The progressing miniaturization in the whole range of electronic device technology necessitates the preparation of nanocrystalline ceramic powders. A quite new method in this field is combustion synthesis.[11,12] A solid mixture which contains oxidizing and reducing reactants is ignited thermally and a fast redox reaction takes place which produces a lot of gases and the desired ceramic powder as the only solid product. The advantages of this method are mainly its low cost — metal nitrates and mostly NH_4NO_3 are used as the oxidizing reactants and e.g. urea, dihydrazides or carboxylic acids like ethylene diammine tetraacetic acid (EDTA) as the reducing reactants — and its simpleness because of the use of aqueous solutions of these reactants which only have to be evaporated to form the solid ignition mass. One can influence the products properties by changing parameters like the characteristics and total amounts of oxidizing and reducing reactants, their ratio or the ignition temperature. Thus, this method is a very versatile tool to produce nanosized powders of almost any desired product.

* Corresponding author Tel.: +49-0681-302-2421; fax: +49-0681-302-4233.

E-mail address: hp.beck@rz.uni.sb.de (H.P. Beck).

0955-2219/00/$ - see front matter
PII: S0955-2219(99)00189-2

In the first part of this paper,[13] the influences of these parameters on the ignition products were examined for the synthesis of $SrTiO_3$. In this second part, the sintering behaviour of such nanocrystalline powders at low temperatures (800 and 1000°C) i.e. the crystallite growth velocities and the formation of impurities and their decomposition is examined.

2. Experimental

A detailed description of the preparation method and the properties of the ignition products (abbreviated as IP in the following) is given in part one, only a short overview will be given here.

The educt mixtures contained $Sr(NO_3)_2$, $TiO(NO_3)_2$, NH_4NO_3 and EDTA; the nitrate groups are the oxidizing and the ammonium groups and EDTA the reducing reactants. Five different mixtures were examined, the compositions were:

I:	Sr:	Ti:	EDTA 1:1:1,	7 NH_4NO_3
II:	Sr:	Ti:	EDTA 1:1:1,	15 NH_4NO_3
III:	Sr:	Ti:	EDTA 1:1:2,	7 NH_4NO_3
IV:	Sr:	Ti:	EDTA 1:1:2,	25 NH_4NO_3
V:	Sr:	Ti:	EDTA 1:1:2,	40 NH_4NO_3

Aqueous solutions of these components were evaporated on a heater plate and the solid obtained was kept in a drying oven for 4–6 h at ~120°C. The resulting brown, brittle masses were ignited in a corundum crucible preheated to an ignition temperature (abbreviated as iT in the following) in a muffle furnace at ambient atmosphere.

The reactivity of the mixtures, i.e. the violence of the ignition reaction, decreases with decreasing ratio of oxidizing to reducing reactant and for same ratios with increasing dilution of the metal cations in the combustible matrix. Thus the reactivity increases in the sequence III < I < IV < V < II. Except for the very reactive mixtures V and II which already at low iT produce more heat during reaction than can be dissipated by the gases evolved, the reaction becomes more violent and faster with higher ignition temperature.

An example for an 'ideal' reaction taking only the components of the mixture into account could be formulated as:

$$Sr(NO_3)_2 + [TiC_{10}H_{12}N_2O_8] + 15\,NH_4NO_3 \Longrightarrow SrTiO_3 + 10\,CO_2 + 17\,N_2 + 36\,H_2O$$

However, deviations will occur due to incomplete pyrolysis of some educts and because of the participation of air in the oxidizing process. Factors governing the reactivity, the nature of the raw products and changes in composition have been described before. The experiments reported here should show the development of crystal growth and impurity contents.

To this aim, these products were sintered as uncompacted powders at 800 resp. 1000°C in a corundum crucible at ambient atmosphere for varying times. At these fairly low temperatures, no liquid phases can occur, and the powders remain in submicron size.

X-ray diffraction data were taken on a Siemens D5000 diffractometer with Cu/$K_{\alpha 1}$ radiation. The resulting diffraction patterns were refined with the program FORMFIT,[14] a detailed description is given in part one of this paper. Fourier-transform infrared-spectroscopy (FTIR) was done with a Perkin–Elmer Spectrum 2000 in the IR-region from 4000 to 400 cm^{-1} on the undiluted compacted powders in diffuse reflectance. For gas adsorption experiments, the powders were kept in an desiccator which was flooded with small amounts of the corresponding gases after slight evacuation. The specimens were not modified before thermally or by vacuum treatment in order to observe the adsorption behaviour of the original surfaces. Thermogravimetry combined with mass spectroscopy (TG/MS) measurements were taken on a Netzsch STA 409 under helium atmosphere.

3. Results

The results of the analysis and refinement of X-ray diffraction patterns of the raw products of the combustion procedure are given in Table 1. One can classify these products in four different groups:

- Group 1: products with relatively high contents of $SrCO_3$, Sr_2TiO_4, amorphous TiO_2 and unburned residues.
- Group 2: products with low contents of this kind, but very high microstresses and large lattice parameters compared with those of $SrTiO_3$ single crystals.
- Group 3: mainly amorphous products.
- Group 4: products with good crystallinity and low levels of amorphous phases and impurities.

If one looks at the crystallite sizes of the products, it is at first right surprising that there is no clear correlation with the ignition temperature. One should expect that the crystallite size increases with increasing iT because the higher temperature should enhance sintering of the crystallites. But higher iT also means that the reaction accelerates and gas evolution increases, which hinders sintering. A more detailed approach dealing with the combination of these factors and explaining their results is given in part one of this paper.

Evidently, products with properties varying in a wide range are accessible by simple changes in the composition of the educt mixtures and by different ignition temperatures. It could be expected that these products would show different sintering behaviour. We have, therefore, examined the effect of sintering at 800 and 1000°C where liquid phases will hardly play a role and the powders remain in submicron size. One must keep in mind that the powders were sintered in uncompacted form, thus the different agglomeration rates resulting from the ignition process could play a role. Educt mixtures with high combustible contents and high reactivity undergo a more violent reaction with much higher gas evolution rates than mixtures with smaller combustible contents and lower reactivity. This leads to dust-like products for a violent ignition process and foamy powders for less violent ones, such foamy products are comparable to sol–gel-processed powders and, therefore, more agglomerated. One should expect that higher agglomeration enhances crystallite growth, but there is no correspondence at all. An influence of the agglomeration of the ignition products on crystallite growth can be excluded by the behaviour of the samples in this work.

3.1. Sintering temperature 800°C

3.1.1. X-ray diffraction

The results of refinement of X-ray-diffraction patterns for different products after sintering for 2 resp. 24 h at 800°C are given in Table 2.

Except for the mainly amorphous products, the crystallite growth proceeds only slowly. The difference in growth velocity is visualized in Fig. 1 for the IPs of mixture IV which had undergone different iT; the growth rates decrease with decreasing amorphous content. For comparison the sintering behaviour of the mainly amorphous IP of mixture III, iT 600°C is shown in Fig. 2. In this case the crystallite growth proceeds even faster when the specimen is pretreated at 600°C for 2 h.

Crystalline impurities like $SrCO_3$ and Sr_2TiO_4 decompose slowly because of the relatively low temperature and have disappeared only after 24 h. The changes in the widths of the crystallite size distributions depend more or less on the crystallite growth velocity. The higher this velocity is, the faster is the narrowing of the distribution width. The reduction of microstresses also progresses slowly and seems to stop at a value of a little less than 0.1%. At 800°C sintering temperature, this value is not yet reached by the sintered specimens of IPs with high impurity or microstress levels, only prolonged sintering at this temperature would result in the value mentioned above. Amorphous, unburned residues resulting from an incomplete pyrolysis during ignition are already totally burned out after 2 h.

Table 1
Crystallographic parameters of different ignition products

Mixt/iT	Δm (%)[a]	a (pm)[b]	D_v (nm)[c]	e (%)[d]	σ[e]	Group[f]
I/400°C	21	—[g]	—	—	—	I
I/600°C	16	—	—	—	—	I
I/800°C	8	391.05(1)	24	0.34(1)	1.73	I
I/900°C	4	390.59(2)	14	0.04(1)	>>2	IV
I/1000°C	<2	390.63(1)	36	0.13(1)	>>2	IV
II/400°C	2	391.99(2)	26	0.43(1)	1.65	II
II/600°C	<2	391.29(2)	30	0.36(1)	1.66	II
III/600°C	44	Amorphous				III
III/900°C	8	390.54(1)	31	0.11(1)	1.86	—
IV/400°C	33	Amorphous				III
IV/600°C	22	390.63(3)	28	0.28(4)	>2	III
IV/800°C	4	390.70(2)	18	0.36(1)	>>2	IV
IV/900°C	<2	390.66(1)	42	0.17(1)	1.53	IV
V/400°C	14	390.54(1)	26	0.22(1)	>>2	IV
V/600°C	6	390.54(1)	31	0.19(1)	>>2	IV
V/800°C	<2	390.60(1)	20	0.23(1)	>>2	IV

[a] Δm: Thermogravimetric weight loss of the product under ambient atmosphere up to 1200°C.
[b] a: Lattice constant; compared with single crystal 390.55 pm.
[c] D_V: Medium volume weighted crystallite size.
[d] d: Medium microstresses.
[e] σ: Width of the crystallite size distribution for an assumed log-normal-distribution; annotations in Discussion.
[f] Group: Assignment to the product groups given in results.
[g] —: High uncertainty of the refined values, no useful results values in brackets are the estimated standard deviation for the last digit.

Table 2
Crystallographic parameters of different ignition products[a]

Mixture/iT [°C]	2 h 800°C D_V [nm], e, [%], σ	24 h 800°C D_V [nm], e [%], σ
I/400	37/0.20/1.7	58/0.16/1.36
I/600	51/0.18/1.48	58/0.13/1.42
I/800	28/0.21/1.66	42/0.13/1.56
I/900	23/0.05/1.67	31/0.09/1.65
I/1000	39/0.11/~2	50/0.12/1.70
II/400	44/0.24/1.36	49/0.22/1.28
III/600	48/0.09/1.53	59/0.06/1.42
III/600	2 h 600°C: 57/0.19/1.53	+24 h 800°C: 111/0.14/<1.2
III/900	47/0.07/1.53	55/0.04/1.33
IV/400	64/0.12/1.40	97/0.08/<1.2
IV/600	57/0.10/1.37	79/0.08/1.34
IV/800	32/0.10/1.86	44/0.04/1.71
IV/900	44/0.11/1.52	60/0.06/1.46
V/400	45/0.04/1.73	59/0.05/1.60
V/600	45/0.10/1.79	50/0.07/1.54

[a] The determination of σ-values for specimens with narrow distributions widths turned out to be difficult. The contributions of the instrument to the diffraction reflection shapes were deconvoluted by measuring LaB_6 as reference substance; a more detailed approach is given in part one of this paper. Slopes of $SrTiO_3$-reflections for specimens with crystallite sizes of ~50 nm and more with low microstresses and narrow size distribution widths were higher and the reflections showed smaller tails than LaB_6 although their FWHMs were always clearly higher. Thus σ-values of ~1.4 and smaller are more and more too low the smaller they are.

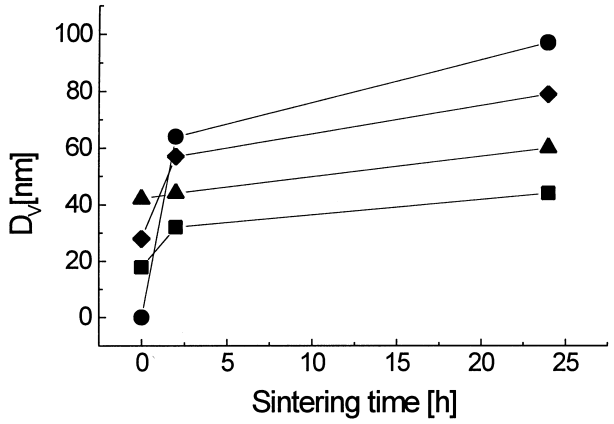

Fig. 1. Development of crystallite size by sintering of the IP of mixture IV at 800°C iT: ●, 400°C; ◆, 600°C; ■, 800°C; ▲, 900°C.

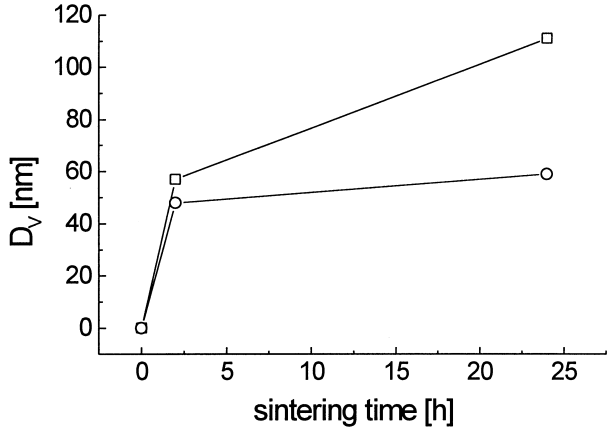

Fig. 2. Development of crystallite size by sintering of the IP of mixture III, iT 600°C, at 800°C; □, 2 h 600°C; +22 h 800°C; ○, 24 h 800°C.

3.1.2. FTIR-spectroscopy

Since FTIR-spectra were taken on the undiluted powder in diffuse reflectance, a very high sensivity for strongly absorbing species such as carbonate or nitrate groups was achieved. The spectra therefore exhibit the existence of carbonate species in the products even for 'X-ray pure' powders which show only negligible weight loss in thermogravimetry. Adsorbed water is also indicated by spectroscopy as well as surface- and bulk-hydroxygroups. None of the ignition products exhibited peaks which could be attributed to nitrate groups. The spectra were taken from 4000 to 400 cm^{-1}, but only the range between 2000 and 1000 cm^{-1} proved to be of special interest.

Figs. 3 and 4 show examples of spectra of different products. The specimens chosen here were those of an IP with fast (mixture III, iT 600°C) and of two with a slower crystallite growth (mixture I and IV, both iT 900°C). The spectra of the original IPs are shown in Fig. 3 except for that of mixture III; this is black because of

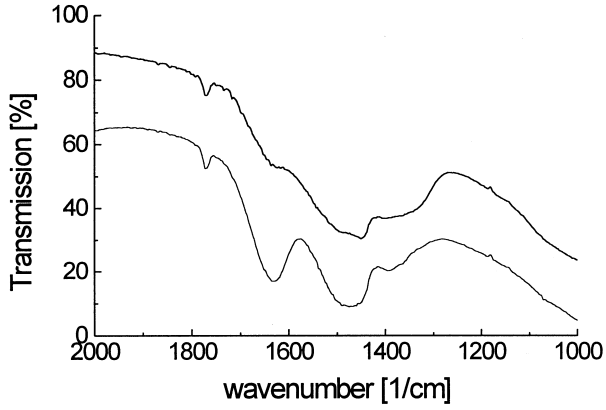

Fig. 3. FTIR-spectra of the IP of mixture I (bottom) and mixture IV (top), both iT 900°C.

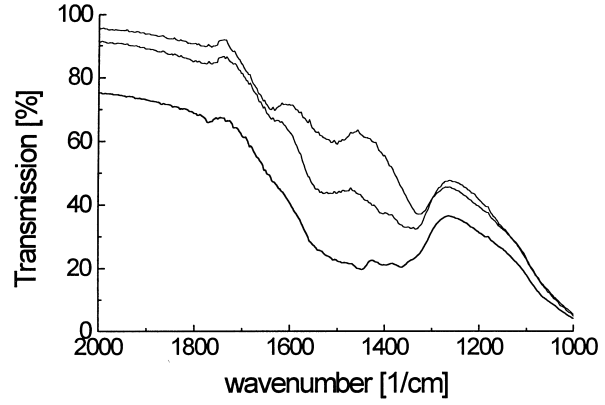

Fig. 4. FTIR-spectra of mixture III, iT 600°C (bottom), mixture I and IV, both iT 900°C (middle and top), all 24 h sintered at 800°C.

high amounts of unburned carbon resulting from the low nitrate content in the ignition mixture, and it therefore absorbed the radiation over the whole frequency range. Fig. 4 shows the spectra of the corresponding specimens after 24 h sintering at 800°C.

The amounts of adsorbed water decrease with increasing sintering time and the corresponding peaks around 1635 cm^{-1} have almost disappeared after 24 h. The same accounts for the surface hydroxygroups in the region between ~3700 and 3400 cm^{-1}. The intensities of peaks between ~3400 and 3100 cm^{-1} which have been attributed to OH-groups contained in the bulk decrease more slowly and there is always a residue of such groups after 24 h of thermal treatment.

The carbonate peaks of the IP are very intense and broad, and contrary to the adsorbed water and the hydroxygroups, they show differences in the decomposition behaviour for different specimens. The amount of carbonate species is strongly reduced by sintering, but while the IP of mixture I shows no more absorbance in the carbonate region except for a peak at ~1322 cm^{-1}, the other samples still exhibit different carbonate species in the whole region between 1600 and 1300 cm^{-1}. An assignment for these peaks will be given in the discussion.

At this sintering temperature, the only connection between crystallite growth rates and the decomposition behaviour especially of carbonate groups is the fact that samples with higher growth rates still show carbonate peaks after one day of sintering. This will gain more interest in the following sections.

3.2. Sintering temperature 1000°C

3.2.1. X-ray diffraction

Table 3 shows the results of refinements of X-ray diffraction patterns of samples treated for 1, 4 and 24 h at 1000°C. Products of group IV show crystallite growth rates somewhat higher than at 800°C, but their growth is the slowest compared to the products of other groups. The highest growth rates are found for products of groups I and II, group III products show almost the same growth rates as at 800°C. Fig. 5 shows the crystallite growth for the IPs of mixture I. The higher the amounts of impurities in the IP i.e. the lower the iT was, the faster the crystallite growth proceeds.

Already after 1 h sintering, all crystalline impurities have dissappeared. The microstresses are reduced quickly to a stable value of ~0.03%. The widths of the crystallite size distributions show the same behaviour as for sintering at 800°C; the faster the crystallite growth proceeds, the faster the distribution widths decrease. An exception is mixture III, iT 900°C. Due to the strongly reducing conditions during the ignition — brought about by the low nitrate content compared to the amount of organic matrix — this product is partly metallic-blue. This indicates the existence of reduced titanium species. The abnormal growth velocity at the beginning of the sintering process therefore cannot be compared to the growth behaviour of other samples.

3.2.2. FTIR-spectroscopy

In contrast to the results of FTIR-spectroscopy on samples sintered at 800°C, there now is a clear dependence between crystallite growth rates and the decomposition behaviour of carbonate groups as seen in FTIR-spectra. Figs. 6 and 7 show typical examples for such spectra. A specimen with slow crystallite growth is shown in Fig. 6 (mixt. I, iT 900°C); already after one hour, there is only one peak at 1322 cm^{-1} left except for those showing small amounts of adsorbed water. Fig. 7 gives the spectra for an IP showing faster crystallite growth (mixture I, iT 400°C). A peak at 1448 cm^{-1} is still visible after 4 h

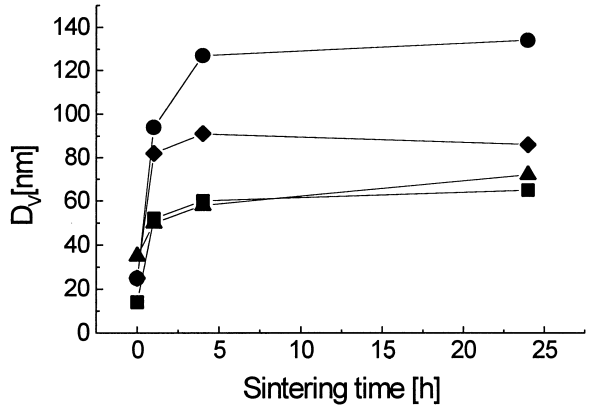

Fig. 5. Development of crystallite size by sintering the IP of mixture I at 1000°C iT: ●, 400°C; ◆, 600°C; ■, 900°C; ▲, 100°C.

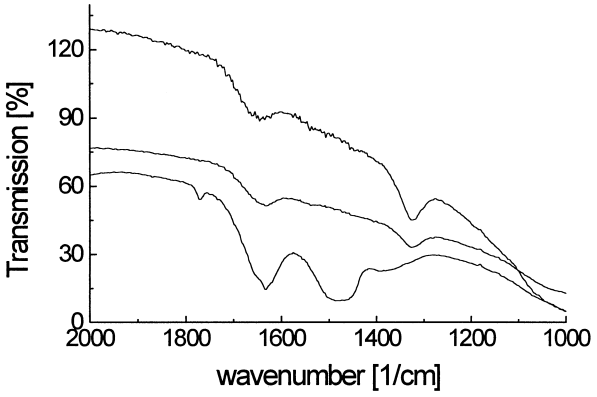

Fig. 6. FTIR-spectra of mixture I, iT 900°C. From bottom to top: IP, 1 h, 24 h sintered at 1000°C.

Table 3
Crystallographic parameters of different ignition products[a]

Mixt./iT (°C)	1 h 1000°C D_V (nm), e (%), σ	4 h 1000°C D_V (nm), e (%), σ	24 h 1000°C D_V (nm), e (%), σ
I/400	94/0.03/1.30	127/0.05/1.20	134/0.03/<1.2
I/600	82/0.09/1.29	91/0.09/<1.2	86/0.06/1.28
I/900	52/0.03/1.50	60/0.05/1.46	65/0.03/1.33
I/1000	50/0.04/1.60	58/0.02/1.49	72/0.03/1.33
II/400	75/0.13/<1.2	141/0.05/<1.2	154/0.04/<1.2
II/600	107/0.06/<1.2	112/0.04/<1.2	140/0.03/<1.2
III/900	95/0.03/1.33	109/0.02/<1.2	120/<0.02/<1.2
IV/400	69/0.11/1.30	75/0.09/1.33	72/0.07/1.30
IV/800	51/0.05/1.49	59/0.05/1.45	66/0.02/1.40
IV/900	—	66/0.03/1.38	69/0.03/1.32
V/400	49/0.04/1.60	58/0.06/1.54	61/0.04/1.42

[a] Explanation see Tables 1 and 2.

and even becomes more intense after 24 h sintering. Another even clearer example for the development of carbonate peaks after longer sintering times is shown in Fig. 8 (mixture IV, iT 800°C). After one day, there is again only the peak at 1322 cm^{-1}, but after 4 days sintering, peaks at 1450 and 1486 cm^{-1} have developed additionally. This phenomenon occurs for numerous specimens after longer sintering at 1000°C.

The behaviour of surface- and bulk-hydroxylgroups is as expected: their decomposition proceeds faster than at 800°C, and surface hydroxyls are faster decomposed than bulk hydroxyls.

3.2.3. Thermoanalysis

TG/MS-data were taken for specimens showing different kinds and intensities of peaks in the carbonate region. Fig. 9 shows an TG/MS-run for mixture I, iT 900°C, 24 h at 1000°C (see Fig. 5). A broad peak in the MS-trace showing the evolution of CO_2 between 300 and 550°C is seen, but the total amount of CO_2 evolved is too low to be determined by TG. The rising background is a typical feature of the instrument, for quantitative determinations (not done here), it could be subtracted by measurements with empty crucibles. A TG/MS-run for the specimen discussed in Fig. 7 after 4 days sintering at 1000°C is given in Fig. 10. An additional desorption between 550 and 700°C is detected which seems to correspond with the peaks at 1450 and 1486 cm^{-1}. Other TG–MS-runs on various samples confirm these statements.

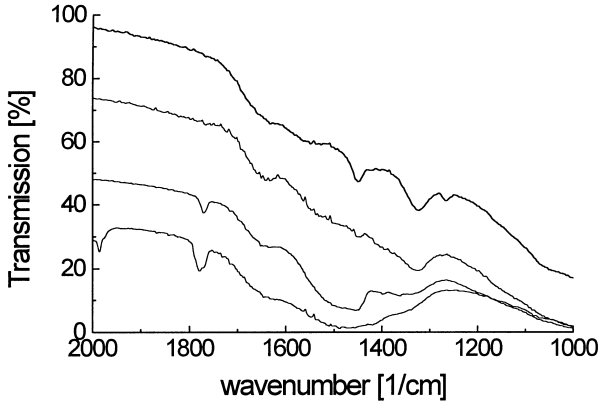

Fig. 7. FTIR-spectra of mixture II, iT 400°C. From bottom to top: IP, 1 h, 4 h, 24 h sintered at 1000°C.

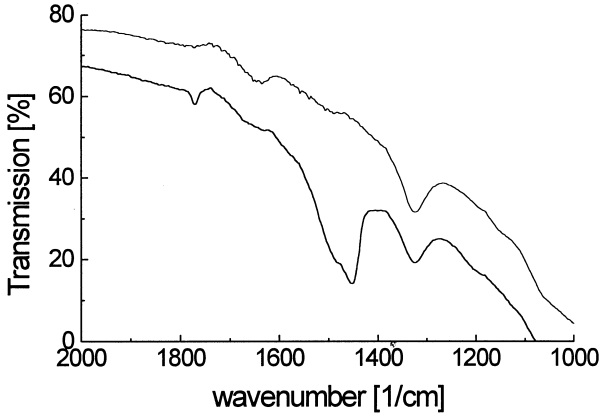

Fig. 8. FTIR-spectra of mixture IV, iT 800°C, after 24 h (top) and 96 h (bottom) sintering at 1000°C.

4. Discussion

The sintering and adsorption behaviour of nanocrystalline powders with low agglomeration as described in this paper are determined by the crystallite surfaces. For $SrTiO_3$ and other perovskites with valencies +2 and +4 for the A- and the B-cation, the electroneutral (100)-faces are the most stable surface terminations, and they therefore predominate. These faces can be terminated either by an AO- or a BO_2-plane. Almost all authors of such studies on the surfaces of perovskite type ceramics confirm that AO-layers dominate the surfaces because of the lower polarization effect of the A-cation compared to the smaller B-cation with higher valency. This accounts for both single crystals[15,16] and polycrystalline samples.[17–19]

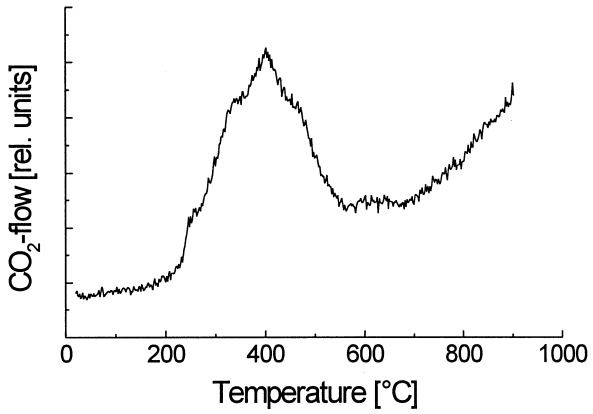

Fig. 9. TG/MS-run of mixture I, iT 900°C, 24 h sintered at 1000°C.

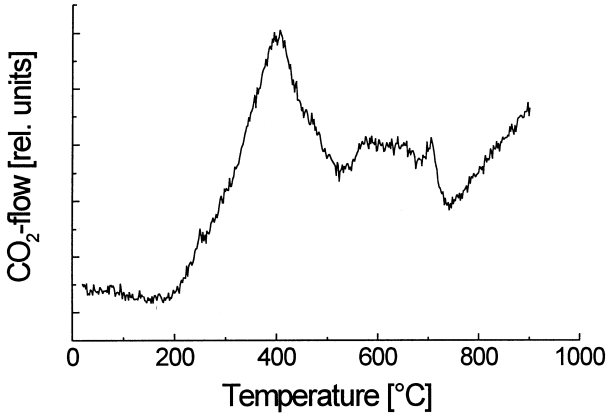

Fig. 10. TG/MS-run of mixture IV, iT 800°C, 96 h sintered at 1000°C.

A simple method to determine the surface termination is to examine the surface acidity. This is mostly made by adsorbing gaseous pyridine on the samples and examining the change in its absorption frequencies in the infrared region. The peak whose wavenumber changes most upon absorption lies at 1584 cm^{-1} in liquid pyridine and shifts to 1593 cm^{-1} on CaO and to 1608 cm^{-1} on both rutile and anatase.[17–20] The higher the Lewis-acidity of the cation is, the more this peak is shifted. FTIR-spectra of ignition products and of samples after sintering for different times at various temperatures always show this peak between 1592 and 1595 cm^{-1}, the surface acidity is typical for a SrO-termination.

The surfaces can also be characterized by the peaks resulting from either residual carbonate groups or by CO_2-adsorption from the air. Fig. 11 shows the FTIR-spectra of $SrCO_3$ after dilution with KBr in the weight ratio 1:10 and ~1:2000. In the highly diluted sample the most intense peak at 1486 cm^{-1} still has an absorption of ~40% which confirms the high sensitivity of the method for the carbonate ions.

The range between 1800 and 1200 cm^{-1} is zoomed in Fig. 12, the second spectrum is that of SrO prepared by heating $Sr(NO_3)_2$ for 2 h at 1000°C and measured some hours after the end of decomposition. The fact that the spectrum shows the same absorbance as $SrCO_3$ except for bulk vibrations shows the high basicity of SrO. A fast absorption of CO_2 from the air takes place and $SrCO_3$ is formed at the surface. This high basicity causes an immediate CO_2-adsorption on SrO-terminated surfaces in ambient atmosphere. The peaks at about 1440, 1400, 1365 and 1322 cm^{-1} are important in this context. The peaks in this region have been assigned to surface carbonate species whose absorption frequencies are shifted because of the different crystallographic surrounding close to the surface.[17,18]

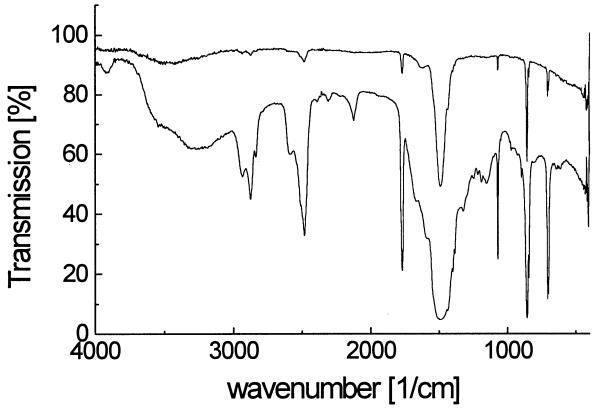

Fig. 11. FTIR-spectra of $SrCO_3$, diluted with KBr in the ratio 1:10 (bottom) and 1:1000 (top).

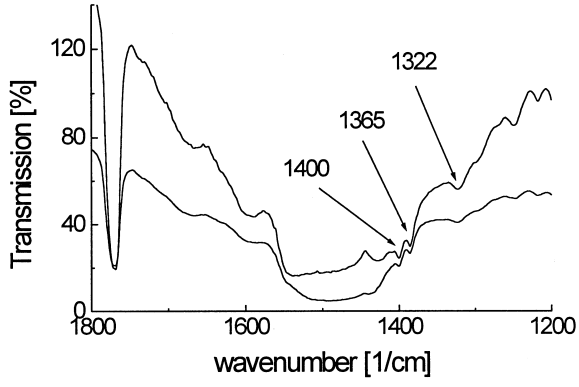

Fig. 12. FTIR-spectra of SrO, undiluted (top) and $SrCO_3$ diluted 1:10 with KBr (bottom).

These wavenumbers are exactly the same as they are seen in the FTIR-spectra of the IPs and of the sintered samples. The peak at 1322 cm^{-1} was at first difficult to explain. It could be compared with that of CO_2 adsorbed on rutile or anatase reported in various other papers.[20] In the course of their studies, the samples were activated by heating in vacuum to desorb the strongly adsorbed water. Our own experiments to adsorb CO_2 or NH_3 on untreated surfaces of TiO_2 were not succesful, not even the very basic NH_3 adsorbed on such samples and the spectra only showed the adsorbed water. These facts indicate that the peak at 1322 cm^{-1} really belongs to a surface $SrCO_3$-species.

This surface species is due to an adsorption of CO_2 from the air and not a residue of carbonate groups resulting from the preparation process. To prove this, a mixture of TiO_2 and $Sr(NO_3)_2$, two acidic materials with no 'intrinsic' carbonate content, was heated for 24 h at 1000°C in air, the FTIR-spectrum of the resulting pure $SrTiO_3$ showed only the peak at 1322 cm^{-1}, i.e. adsorption of CO_2 from air plays a decisive role.

There is also a close relationship between the absorption frequencies in FTIR-spectroscopy and the decomposition temperature at which CO_2 is evolved. The lower the wavenumber, the lower is the decomposition temperature. This leads to the assumption that — simply spoken — the nearer a carbonate group lies to the surface, the lower is its absorption frequency. There probably is a transition from the 'normal' perovskite structure in the bulk to a surface region, where defects of all kind may accumulate and the composition changes to higher SrO-contents. The structural surroundings of the carbonate groups in such SrO-rich regions will change and so will its characteristic frequencies. It is interesting to note that these frequencies are the same encountered in $SrCO_3$ as already described above.

From another point of view, the shift of the carbonate absorption frequencies is an indication for the number of SrO-layers at a surface where CO_2 is adsorbed resp. absorbed. A large number of such layers will incorporate CO_2 as bulk-$SrCO_3$, on thin SrO-layers only surface-carbonate species will form and an adsorption on a single SrO-layer causes the vibration at 1322 cm^{-1}.

The data given in the results show a dependence between crystal growth velocity and the existence and time-dependent behaviour of the carbonate peaks in FTIR-spectroscopy at least for samples sintered at 1000°C. Samples with slow crystallite growth almost only show the peak at 1322 cm^{-1}, while samples with faster growth rates exhibit more peaks in the carbonate region for a longer time during heat treatment. This means that the SrO-rich regions are thicker and thus help to accelerate crystallite growth.

If the samples have the ideal stoichiometry with a ratio of Sr:Ti of 1:1, SrO-rich regions have to be compensated by TiO_2-rich regions. Such regions can only be formed as segregations in grain boundaries in the form of an amorphous phase because TiO_2 is insoluble in $SrTiO_3$. On the other hand SrO is soluble in $SrTiO_3$ for all ratios up to Sr_2TiO_4 by inserting SrO-layers in [100]-direction. Ordered phases of this kind are the so called Ruddlesden-Popper-phases.[21,22] TiO_2-rich phases could not be found by the means used in this work, whereas SrO-rich phases in surfaces were indirectly accessible by FTIR-spectroscopy. X-ray diffraction exhibited no further phases in the sintered specimens although the signal to noise-ratio was excellent. The reformation of 'thicker' SrO-layers on prolonged heating which can be inferred from FTIR-spectra shown in Fig. 8 is not unexpected. It has been described in several papers. The authors sintered powders of milled single crystals and coarse grained ceramic samples of perovskites and observed a decomposition of the ideal perovskite structure in SrO-rich phases and rutile in ambient atmosphere.[23,24] Other authors sintered single crystals in vacuum and observed a diffusion of SrO to the surface; at first SrO-rich phases were formed and then even clusters of up to 100 nm of pure SrO occured.[15,16] This was confirmed by scanning tunneling spectroscopy (STM) and ultraviolet photoelectron and auger electron spectroscopy (UPS/AES). The fact that we have observed this phenomenon to very different degrees may be explained by the great differences in diffusion paths within the nanocrystalline materials. Longer sintering times would show this effect on all samples.

As a consequence of the results given here the crystallite growth rates for the various IP-groups can thus be explained as follows:

Group I: The slow decomposition of impurities like $SrCO_3$ and Sr_2TiO_4 generates SrO-rich regions, but at 800°C the high levels of microstress and lattice faults hinder the migration of SrO. If the temperature is increased up to 1000°C, these lattice defects decrease quickly, and the grain growth accelerates.

Group II: The growth behaviour of these products is the same as for group I. Since only small amounts of SrO-excess at the crystallite boundaries are necessary to enhance crystallite growth, low levels of impurities like $SrCO_3$ and Sr_2TiO_4 are sufficient to generate such SrO-rich regions by their decomposition.

Group III: Specimens of this group show medium to fast growth at 800°C, a segregation of SrO at the initial state of sintering is possible and supports the growth. The crystallite growth at 1000°C differs between different samples which was confirmed by other samples not mentioned in this work. Most of the powders show high growth rates, but some even sinter more slowly at 1000°C than at 800°C. An explanation for this behaviour could lie in the very beginning of the sintering process. At the higher temperature, a fast development of the ideal, stoichiometric structure from the amorphous starting material becomes more likely. This implies the absence of SrO-rich regions and therefore decreases the growth velocity.

Group IV: These products have a good crystallinity and show smaller amounts of amorphous material. The stoichiometry is nearly ideal, i.e. there are little SrO- or TiO_2-rich regions. The crystallite growth proceeds by normal grain boundary and pore migration mechanisms and the growth velocities therefore are low at these low sintering temperatures. As expected the growth proceeds faster at 1000°C than at 800°C.

As a résumé, one can say that small local deviations from the ideal stoichiometry are decisive for the crystallite growth rates. Such deviations can either occur by the existence of impurities like $SrCO_3$ in the ignition product which are decomposed by thermal treatment or by segregation processes which happen at the beginning of the sintering process. High levels of microstresses and lattice faults decrease the mobility of SrO-rich phases and hinder the sintering process, so the sintering temperature has to be increased to accelerate the growth velocity.

5. Conclusion

The sintering behaviour of $SrTiO_3$-samples prepared by combustion synthesis varies strongly with the properties of the ignition products. Such strong variations caused by only small differences between various samples are typical for nanosized powders, they may be prepared by sol-gel methods or combustion synthesis. Samples of good crystallinity and with both low amorphous and crystalline impurities show the slowest growth velocities. Amorphous products exhibit high growth rates at 800 and somewhat higher ones at 1000°C. Specimens with high amounts of crystalline impurities like $SrCO_3$ and Sr_2TiO_4 and/or high microstresses grow slowly at 800°C and faster at 1000°C. This is a consequence of the existence of SrO-rich regions in the samples which accelerate crystallite growth. Such SrO-rich regions are indicated by different $SrCO_3$-species resulting from an CO_2-adsorption from the air by the strongly basic SrO and can be inspected by FTIR-spectroscopy.

Acknowledgements

This work was supported by the DFG in the frame of the Graduiertenkolleg 'Fundamental principles and technology of new high performance materials' and of SFB 277 'Interface dominated materials'.

References

1. Brook, R.J., Controlled grain growth, In *Ceramic Fabrication Processes. Treatise on Materials Science and Technology Vol.9*, ed. S.S.Y. Wang. Academic press, New York, pp. 1976, 331–369.
2. Bell, A. J., Moulson, A. J. and Cross, L. E., The effect of grain size on the permittivity of $BaTiO_3$. *Ferroelectrics*, 1984, **54**, 147–150.
3. Kinoshita, K. and Yamaji, A., Grain size effects on dielectric properties in barium titanate ceramics. *J. Appl. Phys*., 1976, **47**(1), 371–373.
4. Uchino, K., Sadanaga, E. and Hirose, T., Dependence of the crystal structure on particle size in barium titanate ceramics. *J. Am. Cer. Soc*., 1989, **72**(8), 1555–1558.
5. Heywang, W., Resistivity anomaly in doped barium titanate. *J. Am. Cer. Soc*., 1964, **47**(10), 484–490.
6. Ihrig, H., PTC effect in $BaTiO_3$ as a function of doping with 3d-elements. *J. Am. Cer. Soc*., 1981, **64**(10), 617–621.
7. Ihrig, H., The positive temperature coefficient resistivity of $BaTiO_3$ ceramics as a function of the amount of Ti-rich second phase. *Phys. Stat. Sol. (a)*, 1978, **47**, 437–444.
8. Fujimoto, M., Suzuki, T., Nishi, Y. and Arai, K., Calcium-ion selective site occupation at Ruddlesden-Popper-type faults and the resultant dielectric properties of A-site excess strontium calcium titanate ceramics. *J. Am. Cer. Soc*., 1998, **81**(1), 33–40.
9. Hammer, M. and Hoffmann, M. J., Sintering model for mixed-oxide-derived lead zirconate titanate ceramics. *J. Am. Cer. Soc*., 1998, **81**(12), 3277–3284.
10. Fujimoto, M. and Kingery, W. D., Microstructures of $SrTiO_3$ internal boundary layer capacitors during and after processing and resultant electrical properties. *J. Am. Cer. Soc*., 1985, **68**(4), 169–173.
11. Zhong, Z. and Gallagher, P. K., Combustion synthesis and characterization of $BaTiO_3$. *J. Mat. Res*., 1995, **10**(4), 945–952.
12. Sekar, M. A. and Patil, K. C., Combustion synthesis of fine-particle dielectric oxide materials. *J. Mat. Chem*., 1992, **2**(7), 739–743.
13. Poth, J., Haberkorn, R. and Beck, H.P., Combustion synthesis of $SrTiO_3$ Part I: synthesis and properties of the ignition products. *J. Eur. Cer Soc*., 2000, **20**, 795–799.
14. Haberkorn, R., FormFit — a program for X-ray powder pattern deconvolution and determination of microstructure. *Dudweiler*, 1998.
15. Liang, Y. and Bonnell, D. A., Atomistic structure of reduced $SrTiO_3$(001) surfaces. *Surf. Sci. Lett*., 1993, **285**, L510–L516.
16. Liang, Y. and Bonnell, D. A., Structures and chemistry of the annealed $SrTiO_3$ (001) surface. *Surf. Sci*., 1994, **310**, 128–134.
17. Amores, J. M. G., Escribano, V. S., Daturi, M. and Busca, G., Preparation, characterization and surface structure of coprecipitated high-area Sr_xTiO_{2+x} $(0<x<1)$ powders. *J. Mat. Chem*., 1996, **6**(5), 879–886.
18. Busca, G., Buscaglia, V., Leoni, M. and Nanni, P., Solid state and surface spectroscopic characterization of $BaTiO_3$ fine powders. *Chem. Mat*., 1994, **6**, 955–961.
19. Daturi, M., Busca, G. and Willey, R. J., Surface and structure characterization of some perovskite-type compounds to be used as combustion catalysts. *Chem. Mat*., 1995, **7**, 2115–2126.
20. Busca, G., Sausey, H., Sur, O., Lavalley, J. C. and Lorenzelli, V., FTIR-characterization of the surface acidity of different titanium dioxide anatase preparations. *Appl. Catal*., 1985, **14**, 245–260.
21. Ruddlesden, S. N. and Popper, P., New compounds of the K_2NiF_4 type. *Acta Cryst*., 1957, **10**, 538–539.
22. Ruddlesden, S. N. and Popper, P., The compound $Sr_3Ti_2O_7$ and its structure. *Acta Cryst*., 1958, **11**, 54–55.
23. Szot, K., Freiburg, C. and Pawelczyk, M., Layer structures BaO-$BaTiO_3$ in the region of p-type conductivity on the surface of $BaTiO_3$. *Appl. Phys. A,*, 1991, **53**, 563–567.
24. Szot, K., Pawelczyk, M., Herion, J., Freiburg, C., Albers, J., Waser, R., Hulliger, J., Kwapulinski, J. and Dec, J., Nature of the surface layer in ABO_3-type perovskites at elevated temperatures. *Appl. Phys. A*, 1996, **62**, 335–343.